



Laboratory Testing of an Active Drilling Vibration Monitoring & Control System

Martin E. Cobern & Mark E. Wassell, APS Technology, Inc.

This paper was prepared for presentation at the AADE 2005 National Technical Conference and Exhibition, held at the Wyndam Greenspoint in Houston, Texas, April 5-7, 2005. This conference was sponsored by the Houston Chapter of the American Association of Drilling Engineers. The information presented in this paper does not reflect any position, claim or endorsement made or implied by the American Association of Drilling Engineers, their officers or members. Questions concerning the content of this paper should be directed to the individuals listed as author/s of this work.

Abstract

The deep, hard rock drilling environment induces severe vibrations, which can cause reduced rates of penetration and premature failure of the equipment. Conventional shock subs are useful in some situations, but often exacerbate the problems.

APS Technology is developing a unique system to monitor and control drilling. This system has two primary elements:

- An active vibration damper (AVD) to minimize harmful vibrations, whose hardness is continuously adjusted.
- A real-time system to monitor drillstring vibration and related parameters. This monitor adjusts the damper according to local conditions.

The AVD is designed to have several favorable effects on the time needed to drill a well. By keeping the bit in constant contact with the well bottom, and maintaining the actual weight applied to the bit (WOB) at the optimum level, the instantaneous rate of penetration (ROP) is increased. Additionally, by reducing the levels of vibration throughout the bottomhole assembly (BHA), the operating life of all downhole components (bits, motors, MWD systems, etc.) is increased, thereby reducing the number of trips required for a particular well. These advantages will apply in all wells, but their value increases disproportionately in deep drilling.

An earlier paper¹ reported on the design and modeling of this system. After briefly reviewing these, we present preliminary laboratory tests that illustrate the ability of the AVD to adjust to a range of downhole conditions. Field test prototypes are being designed and built, and will be field tested in 2005.

Introduction

The drilling environment, and especially hard rock drilling, induces severe vibrations into the drillstring. The result of drillstring vibration is premature failure of the equipment and reduced ROP. The only means of controlling vibration with current monitoring technology is to change either the rotary speed or WOB. These changes may move the drilling parameters away from their optimum value and thus may have a negative effect on drilling efficiency.

Shock subs are not a universal solution, as they are designed for one set of conditions. When the drilling environment changes, as it often does, shock subs become ineffective and often result in increased drilling vibrations, exacerbating the situation. As one study² concluded: "Most of the shock subs tested showed a definite reduction in the axial accelerations experienced in the drillstring above the shock sub.... The accelerations at the bit were little affected, but even at the same accelerations the dynamic forces at the bit were probably reduced. Clearly the best place to run the shock sub is near the bit to minimize both axial and lateral accelerations. Even though it provides some benefit in terms of reducing axial vibrations when run at the top of a packed BHA, *it increases the risk of encountering high lateral vibrations when run in this position. These vibrations may cause more problems in terms of fatigue damage than will be offset by the reduction in the axial vibrations.*" [emphasis added.]

Drillstrings develop vibrations when run at critical rotary speeds, and these vibrations are difficult to control due to the strings' long length and large mass. Operating at a critical speed imparts severe shock and vibration damage to the drillstring, fatigues drill collars and rotary connections. Vibrations also cause the drillstring to lift off bottom, reducing ROP. The effect of axial, lateral or torsional (stick-slip or bit whirl) vibration upon drilling have been documented in the laboratory³ and the field^{2,4}

The natural frequencies of the drillstring often fall in the range excited by typical drilling speeds, between 0.5 Hz and 10 Hz depending on the BHA and length of the drillstring (**Figure 1**). There are many sources that excite drillstring vibrations, including bits, motors, stabilizers and drillstring imbalance. For example, a tricone bit imparts a primary excitation frequency of three times the rotary speed. If rotating between 120 and 180 rpm, the excitation frequency is 6 – 9 Hz. Mud motors are also significant sources of excitations on the drillstring. The rotor of the mud motor moves in an eccentric orbit that oscillates several times per revolution. Depending on the lobe configuration of the motor, excitations occur between 1 and 30 Hz. Shocks from bit bounce and collar impacts against the borehole result in higher frequency vibration.

The best situation for a drillstring is to operate below its lowest critical speed. By staying below this first critical speed, the drillstring is not excited by drilling frequencies and the bit maintains contact with cutting surface of the borehole. In **Figure 2**, this safe range is shown as Zone A. In this example, with a fundamental natural frequency of 6 Hz, this zone extends to 4 Hz, corresponding to a rotary speed to 80 rpm or less for a tricone bit. Zone B is the resonant range that results in high levels of vibration. Shock and vibration damage and low ROP occur in this zone. Zone C lies above the first critical speed of the drillstring. Vibrations levels are reduced compared to Zone A and B; however the bit does not maintain continuous contact with the drilling surface, since the natural frequency of the drillstring is lower than the excitations of the bit preventing it from reacting to vibrations. This discontinuous contact with the drilling surface of the borehole greatly reduces the ROP.

Principles of Operation

The AVD consists of electronics that monitor vibrations and other drilling parameters, and a spring-fluid damper that controls the vibration. The damper properties are **continuously modified** to provide optimal damping characteristics for the conditions present. A key innovation in the AVD is the use of magnetorheological fluid (MRF) as the means of varying the damping coefficient of the AVD.

MRF is a "smart" fluid whose viscous properties are changed by passing a magnetic field through it. MRF components have **no moving parts, rapid response times** and **low power requirements**. The damping properties can thus be optimized to detune the drillstring from resonant vibration.

MRF damping is currently being used in such diverse applications as sophisticated automotive suspensions⁵ and earthquake protection systems for buildings and bridges.⁶

The AVD modifies the properties of the BHA in two ways that combine to increase ROP and reduce vibration. First, the damper isolates the drillstring section below the damper from that above it. Second, it optimizes the damping based upon the excitation forces such that vibration is significantly reduced. The combination allows the bit to respond more quickly to discontinuities on the cutting surface, while maintaining the desired surface contact force.

Separating the bit from the rest of the drillstring with a spring-damper assembly reduces the effective mass that must respond to discontinuities of the drilled surface. Reducing the mass *increases the first critical speed* of the drillstring attached to the bit, while the adaptive damping *reduces the magnitude of vibration* at the resonance. This provides a much wider **Zone A**, as shown

in **Figure 3**, which is based on a simple model of the damper. For a tricone bit, **Zone A** now covers a range of 0 – 220 rpm, a significant improvement compared to the 0–80 rpm shown in **Figure 2**.

The practical effect of these changes are shown in the following figures, which are based on BHA models performed with APS's WellDrill™ software. When the damping force is optimized, which for this case is in the range of 200-300 lb.-sec./in., the bit remains in contact with the formation (**Figure 4**), the WOB remains constant (**Figure 5**), bit vibration is essentially eliminated (**Figure 6**), and the ROP increases (**Figure 7**).

Tool Design

An overview of the AVD tool is shown below in **Figure 9**. The tool has many features of a conventional shock sub, including: a stack of Belleville washers to support the weight applied to the bit; bearings to absorb the axial and torsional loads, etc. The key difference is that the damping coefficient is continually adjustable by varying the magnetic field applied to the MRF. The details of the MRF damper design are shown in

Figure 10, [This drawing is of an earlier test piece, but the configuration is essentially unchanged in the prototype tools. The MRF will be in the volume between the mandrel (2) and the housing (1). A series of coils wrapped in the grooves in the mandrel will create bucking fields, which will be strongest in the gaps between the coils. The MRF in these areas will become more viscous as a function of the field strength, thereby varying the damping of the motion of the mandrel relative to the housing. Other aspects of this test piece will be described below.

The MR damper control algorithm utilizes displacement measurements taken in real time during the drilling operation. Based on this information, the damping properties are continuously modified throughout the drilling process. The intent is to both reduce the motion of the bit relative to the well bottom and smooth out the vibrations above the damper. A hardening damper algorithm was developed as the simplest and most robust method to control damping (**Figure 8**). This method increases damping levels as the damper sections displace relative to one another. For small displacements and low WOB, a low level of damping is provided. As the deflection increases, due to higher either WOB or larger vibration levels, the damping is increased. This method was shown analytically to provide proper damping levels over a wide range of conditions with minimal sensor data.

The new prototype design of the AVD tool uses a Belleville spring stack with a compound spring rate. This provides better isolation at various levels of vibration and WOB compared to shock subs having a linear spring rate. This provides increased deflection for the damping module at low levels of vibration and improved support at high levels.

* US Patent #6,257 356 B1; additional patent applied for.

Test Bench

The design of a test bench to evaluate the performance of the AVD was a significant task in itself. A simple vibration table would not suffice.

In operation, the AVD will be supported and loaded by the entire drill string above it. Considerable weight is applied from above, and this loading would have both resilience and damping. The damping will result from the intrinsic damping in the drill string itself, from the hydraulic damping of the drilling fluid and from contact with the borehole walls. At the bit, the driving force is the interaction of the bit and the irregular bottom of the hole. This interaction will have a primary frequency (e.g., triple the rotation rate for a tri-cone bit), but may have other harmonics as well if there is more than one high point on the well bottom. In addition, the well bottom is not completely rigid, but can respond to the bit by flexing or being drilled away. (If not, there would be no point in drilling.)

To simulate these conditions, we designed the test bench shown in **Figure 11**. The prototype (5) is supported by linear bearings (4) on a large load frame (6). At the 'uphole' end, to the left, a large pneumatic cylinder (1) applies a force simulating the loading from the drill string above the tool. The damping of the drill string motion is simulated by two hydraulic cylinders (2) configured to produce adjustable damping. To mimic the driving force of the bit's interaction with the well bottom, a lower assembly (7) is provided. In this assembly, a cam (8) is rotated by a variable speed gear motor (9) at rates simulating the drillstring rotation rate. The cam, which is supported by ball bearings, can have configurations that mimic a variety of degrees of irregularity of the well bottom.

Test Results

The first test performed was a static test, to measure the damping coefficient of the AVD under various stationary conditions. In this test, a mockup of the damper element was mounted on the test stand, and the hydraulic pistons were used to drive a known volume of MRF through the damper with different voltage levels across the magnet circuit. By measuring the pressures and the time required for this flow, the damping coefficient could be derived from the ratio of the force applied to the fluid velocity.

As shown in **Figure 12**, the damping coefficient increases rapidly with applied power, and decreases roughly linearly as the pressure increases. The fluid pressure is proportional to the force applied, and these early results indicated that the damper would be able to support approximately 6,000 lbs. With much of the WOB supported by the spring stack, the damper will be able to provide the necessary damping at typical WOB values. The damping value with the power off, however, was somewhat higher than desired, making the damper too

stiff for some situations. The gaps between the mandrel and housing were then adjusted to optimize the damper response.

In the next phase of testing, the full laboratory prototype, including the Belleville springs and bearings, was mounted in the test bench and driven by the cam. A sample of the results is shown in **Figure 13**, which plots the dynamic stiffness of the AVD as a function of the current applied and the drive frequency. The dynamic stiffness of the damper is a combination of the stiffness of the springs and the variable damping applied by the AVD. This combination is a function of the frequency of the driving vibration. As the applied current increases, the dynamic stiffness of the AVD rises.

The ability of the damper to reduce bit vibration and bit bounce is shown in **Figure 14**, which plots the maximum motion of the damper collar (connected to the bit) relative to the central mandrel, (connected to the upper drillstring). The driving displacement from the cam was 0.7. As the damping is increased, the maximum motion converges toward a level consistent with the bit's remaining in constant contact with the cam (which simulates the irregular bottom of the well). The damper is thus operating as it was designed to.

[*Note:* These figure combines data taken during different setups. The hydraulic damping controls for WOB and string damping were difficult to control and may not *exactly* repeat their settings from run to run. The data in the figures may, therefore, be slightly offset from one frequency to the next.]

Conclusions

Laboratory testing of the AVD indicates that it is capable of providing the variable damping necessary to control bit bounce, maintain uniform WOB and increase drilling ROP. There are several areas that are still under investigation and development, including:

- Increasing the dynamic range of the damper. The approximately 2:1 variation seen in **Figure 13**, while significant, is not repeated under all conditions, and is less than predicted by the modeling. Further refinements of the damper design are being studied and implemented.
- The hardening algorithm must be tested on the laboratory prototype to demonstrate that it performs as it is modeled.
- A field prototype has been designed and is being manufactured, with some parts of its design on hold pending the results of the testing described above.

Once these open issues have been resolved, it is anticipated that a prototype AVD tool will be tested, first in drilling laboratories and then in the field, in the second half of 2005.

Acknowledgments

This effort has been partially funded by the Deep Trek program of the U.S. Department of Energy National Energy Technology Laboratory, Contract DE-FC26-02NT41664. Neither the United States Government nor any agency thereof, nor any of their employees, makes any warranty, express or implied, or assumes any legal liability or responsibility for the accuracy, completeness, or usefulness of any information, apparatus, product, or process disclosed, or represents that its use would not infringe privately owned rights. Reference herein to any specific commercial product, process, or service by trade name, trademark, manufacturer, or otherwise does not necessarily constitute or imply its endorsement, recommendation, or favoring by the United States Government or any agency thereof. The views and opinions of authors expressed herein do not necessarily state or reflect those of the United States Government or any agency thereof.

The authors are grateful for this generous support.

Nomenclature

AVD	=	<i>active vibration damper</i>
BHA	=	<i>bottomhole assembly</i>
LWD	=	<i>logging-while-drilling</i>
MRF	=	<i>magnetorheological fluid</i>
MTBFF	=	<i>mean time between field failures</i>
MWD	=	<i>measurements-while-drilling</i>
ROP	=	<i>drilling rate of penetration</i>
rpm	=	<i>revolutions per minute</i>
WOB	=	<i>weight on bit</i>

Addendum

[**Note:** Between the submission of the written paper and the presentation at the Conference, additional results were obtained, which were significantly improved over those reported in the paper. These results were presented at the conference and are summarized here.]

The marginal results shown in **Figure 13** were considered to result from one of several factors:

- A high 'baseline' impedance from, for example, the oil-filled Belleville springs;
- A change in the viscosity of the MR fluid as a result of heat or working.
- Residual magnetization of the valve components, which would prevent the MR fluid from returning to its original viscosity.

All of these were studied during the past several months, as follows:

- The damper was run 'dry' without oil in the Belleville spring section.
- A viscometer was obtained and modified to include an electromagnet. The viscosity of our 'home-made' MR fluid, with different ratios of iron filings to oil, was measured at different field strengths and compared to the commercial fluid obtained from Lord⁷.

- A precision magnetic fluxmeter with a small diameter probe was used to test the key components of the valve after use.

The results of this testing showed that the contribution of the oil to the overall damping coefficient was negligible. The home-made MR fluid functioned as well as the commercial fluid, and neither showed any significant change in properties. The valve components, however, did retain significant magnetization after use. This was considered to be the primary source of the lack of dynamic range in the damper.

The control circuit was modified to add a demagnetization field whenever the field was made to decrease.⁸ The effectiveness of this approach can be seen in **Figure 15**, which shows little if any difference between the dynamic stiffness of the AVD before and after it was subjected to the full magnetic field. The demagnetization had a dramatic influence on the dynamic range of the AVD, which can be seen in **Figure 16**.

The AVD can instantaneously vary its dynamic stiffness by a factor of 7-10, depending upon the excitation frequency. This is more than adequate to obtain the results described earlier in the paper. Work is continuing on refining the valve design and implementing the automatic feedback algorithms.

References

- ¹ Martin E. Cobern & Mark E. Wassell, "Drilling Vibration Monitoring & Control System," presented at the National Gas Technologies II Conference, Phoenix, AZ, 8-11 February, 2004.
- ² T.M. Warren, J.H. Oster, L.A. Sinor, and D.C.K. Chen, "Shock Sub Performance Tests," **IADC/SPE 39323**, presented at the 1998 IADC/SPE Drilling Conference, Dallas, March 3-6, 1998.
- ³ *cf.*, e.g., M.W. Dykstra, D.C.-K. Chen, T.M. Warren & S.A. Zannoni, "Experimental Evaluations of Drill Bit and Drill String Dynamics," **SPE 28323**, presented at the 61st SPE ATCE, New Orleans, September 25-28, 1994
- ⁴ *cf.*, e.g., S.L. Chen, K. Blackwood and E. Lamine, "Field Investigation of the Effects of Stick-Slip, Lateral and Whirl Vibrations on Roller Cone Bit Performance," **SPE 56439**, presented at the 58th SPE ATCE, Houston, October 3-6, 1991.
- ⁵ *cf.*, e.g., "Magnetic Ride Control," *GM Tech Links*, Vol. 4, No.1, pp. 1-2, January, 2002, http://service.gm.com/techlink/html_en/pdf/200201-en.pdf.
- ⁶ B.F. Spencer Jr., S.J. Dyke, M.K. Sain and J.D. Carlson, "Phenomenological Model of a Magnetorheological Damper," *Journal of Engineering Mechanics*, ASCE, **123** 230-238, 1997, http://www.nd.edu/~quake/papers/MRD_Journal.pdf.
- ⁷ <http://www.lord.com/Default.aspx?alias=www.lord.com/mr>
- ⁸ R.M. Knight, "How to Demagnetize a Submarine," presented at Meeting #1579 of the Fortnightly Club of Redlands, CA, January 2, 1997. <http://www.redlandsfortnightly.org/subm.htm>

FIGURES

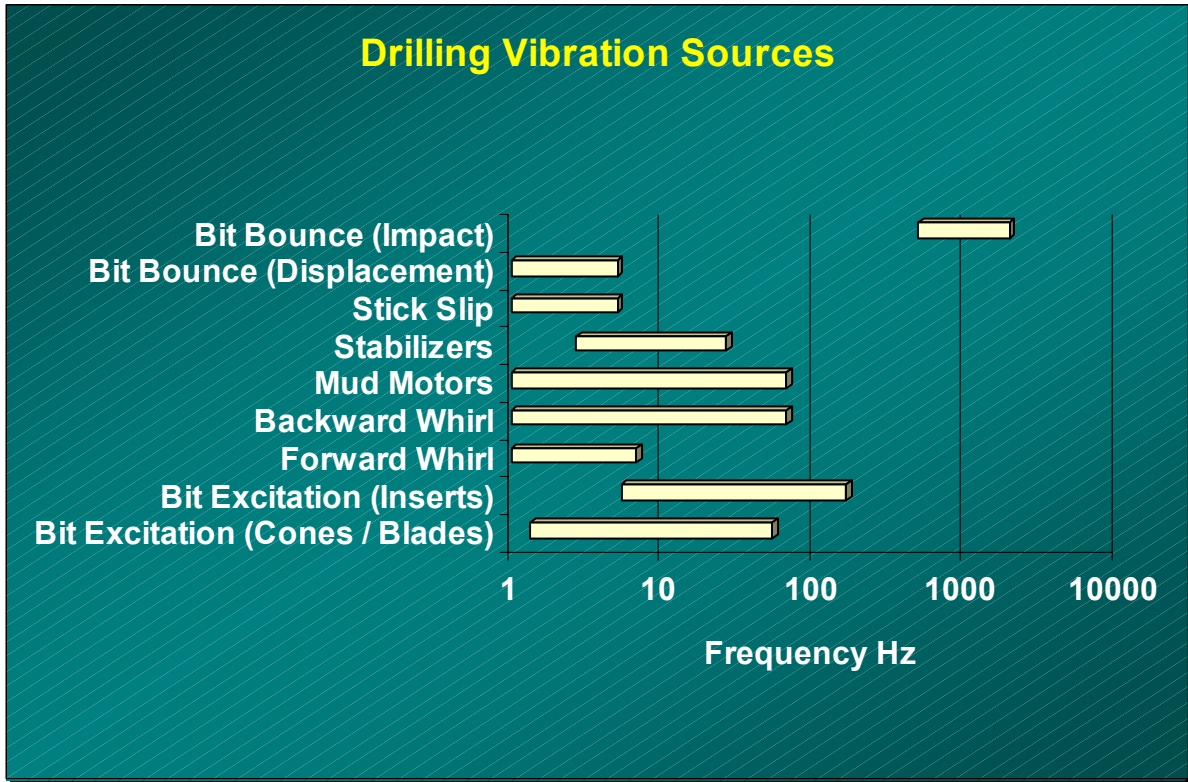


Figure 1 - Drilling Vibration Sources

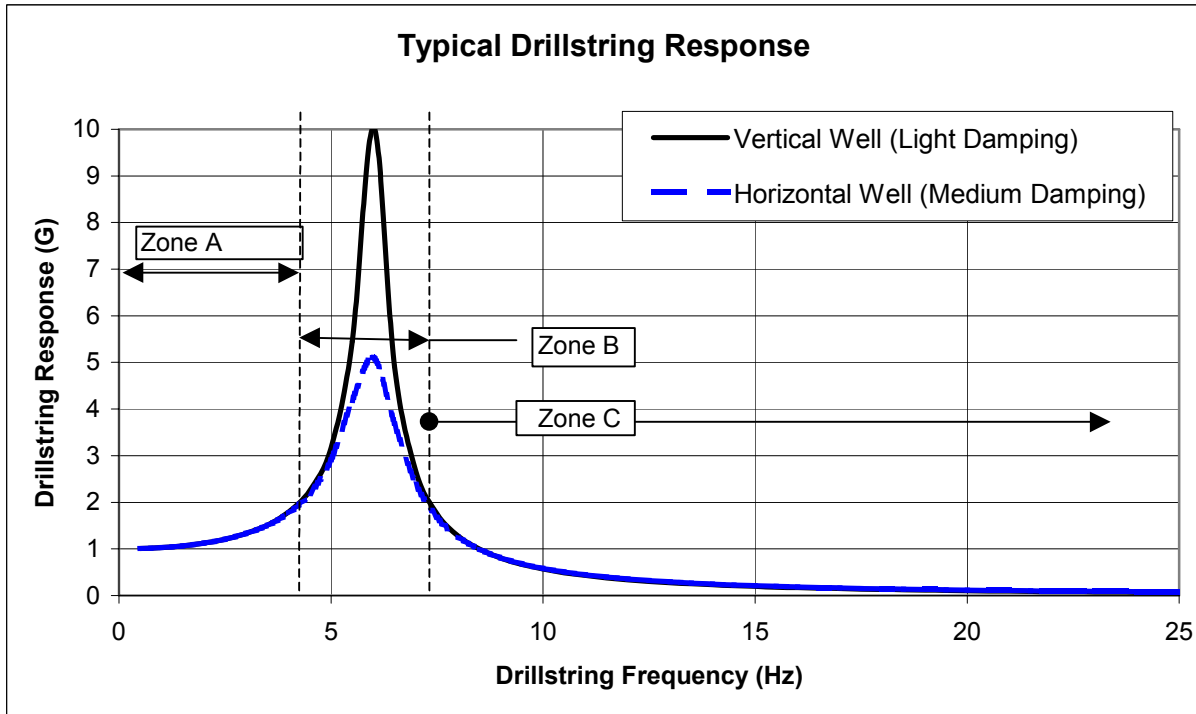


Figure 2: Frequency response of typical drillstring

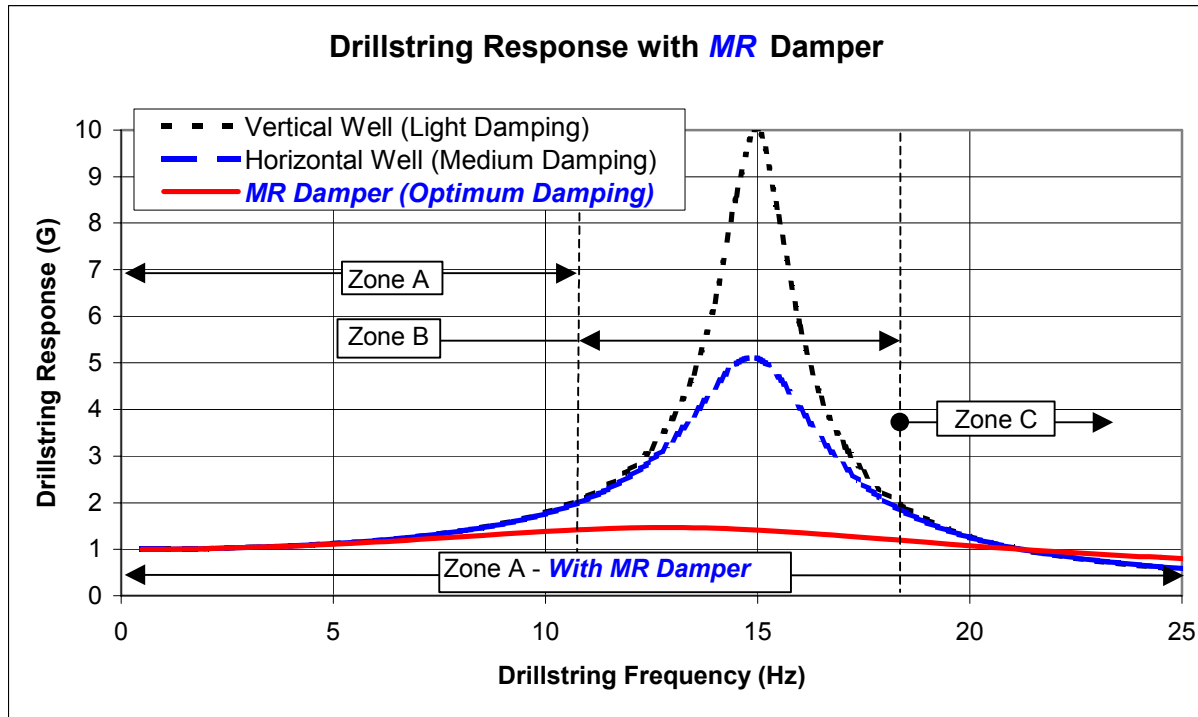


Figure 3: Drillstring response with an AVD in use

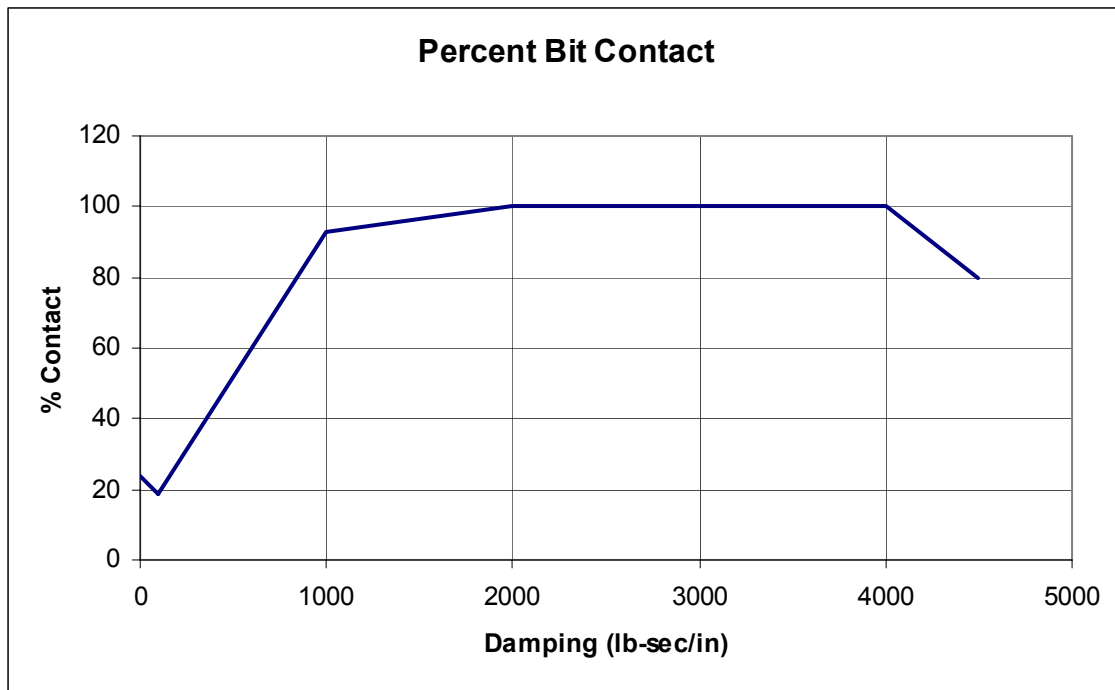


Figure 4: Bit contact : 30,000 WOB - 30,000 in-lb Spring Rate

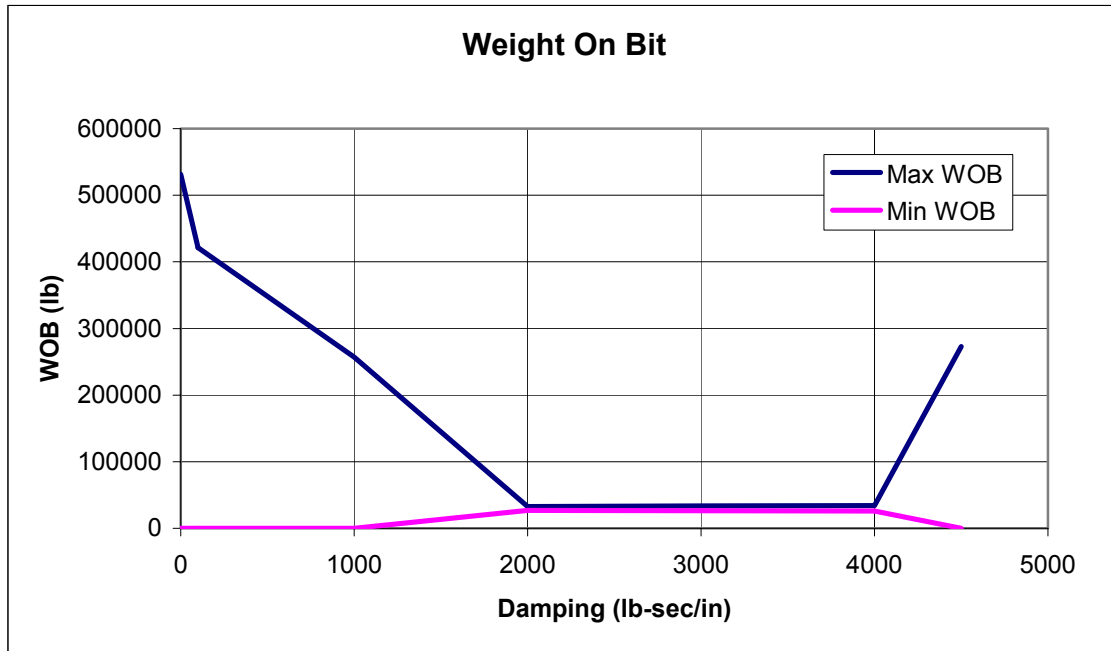


Figure 5: Measured WOB: 30,000 WOB - 30,000 in-lb Spring Rate

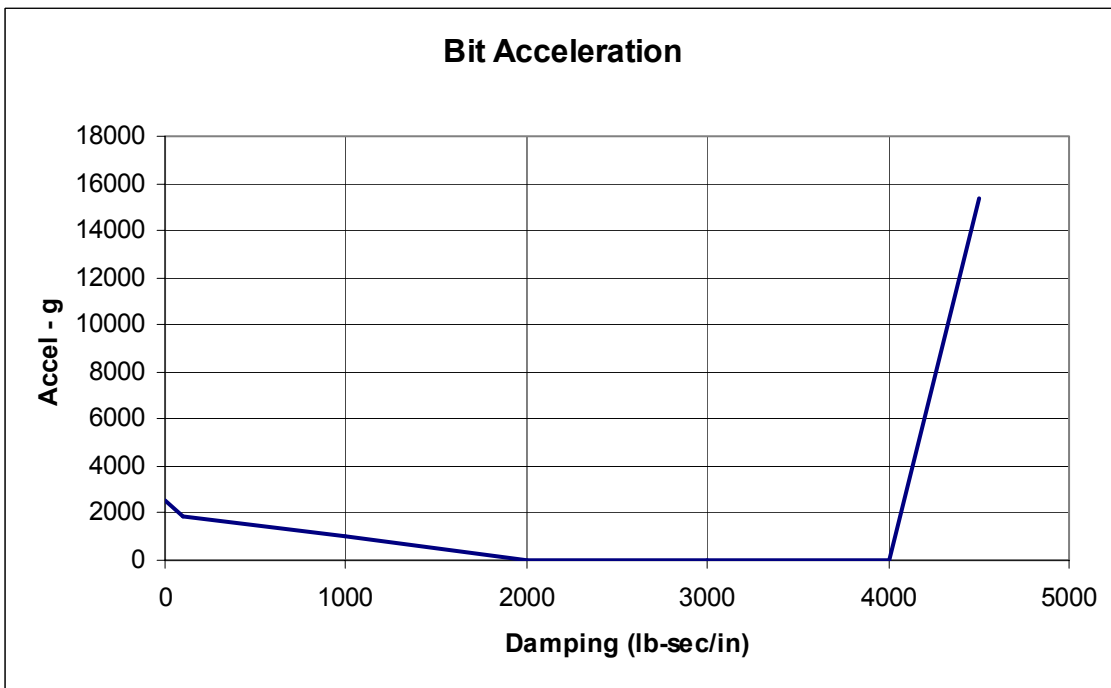


Figure 6: Bit acceleration: 30,000 WOB - 30,000 in-lb Spring Rate

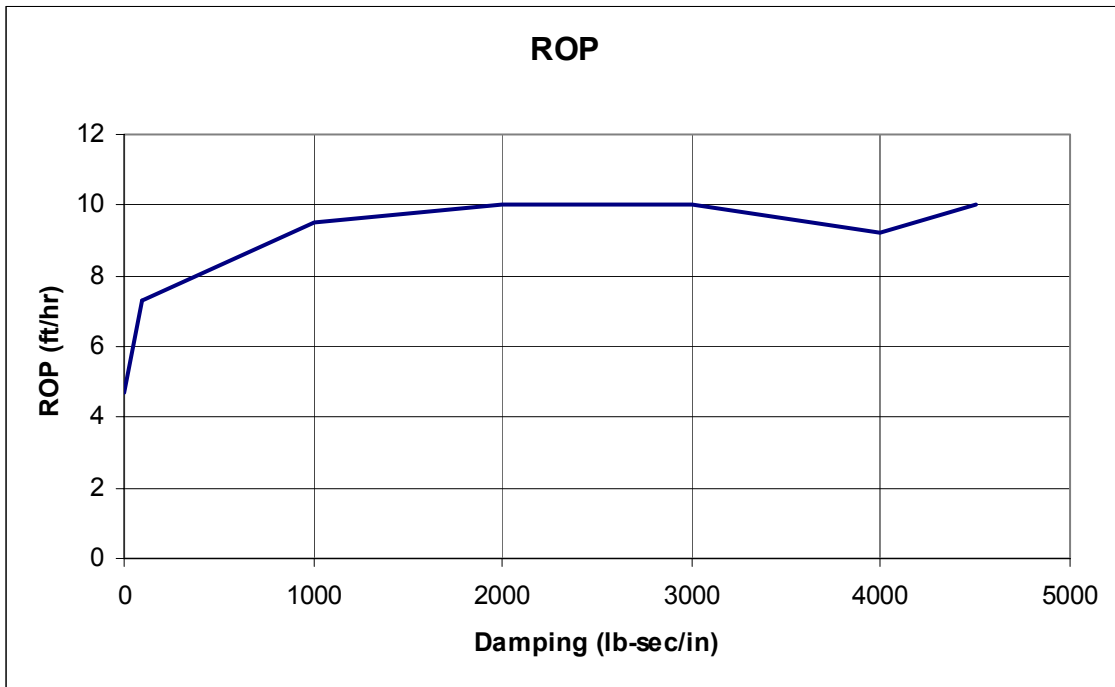


Figure 7: ROP: 30,000 WOB - 30,000 in-lb Spring Rate

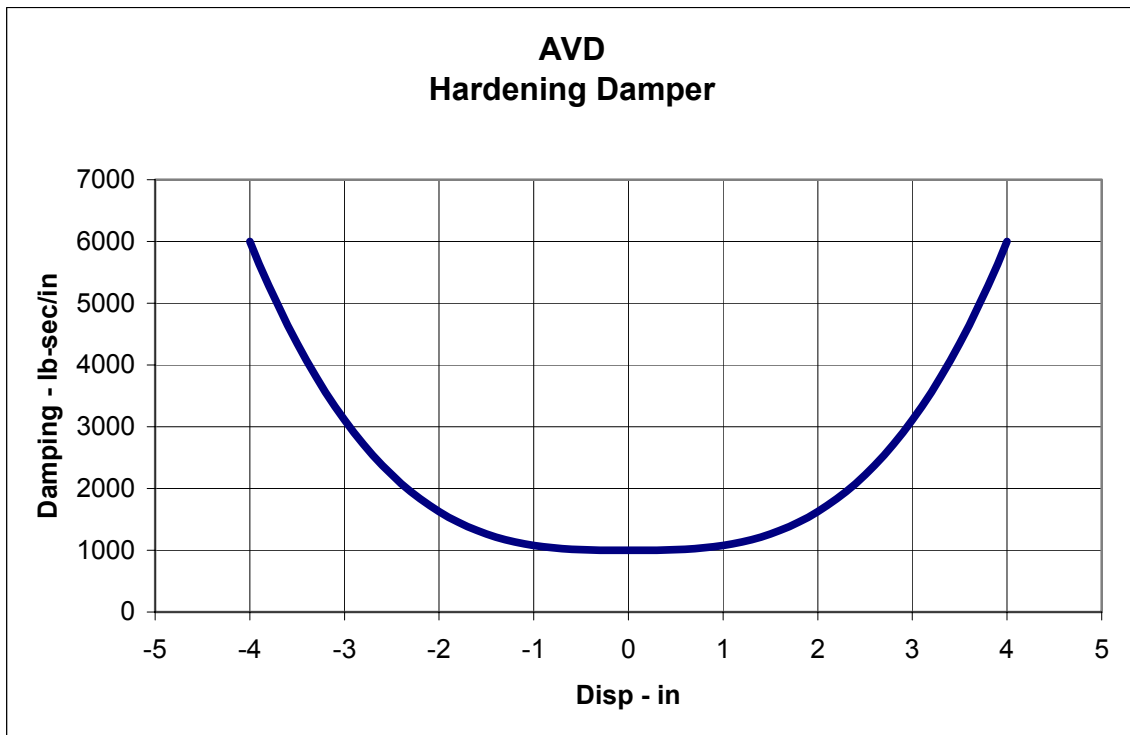


Figure 8 - AVD Hardening Damper

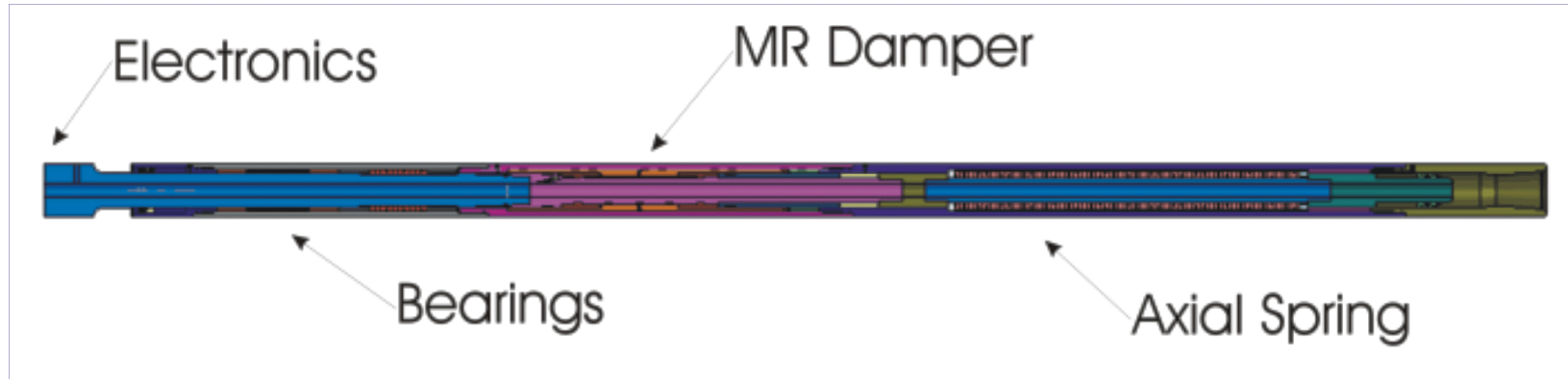
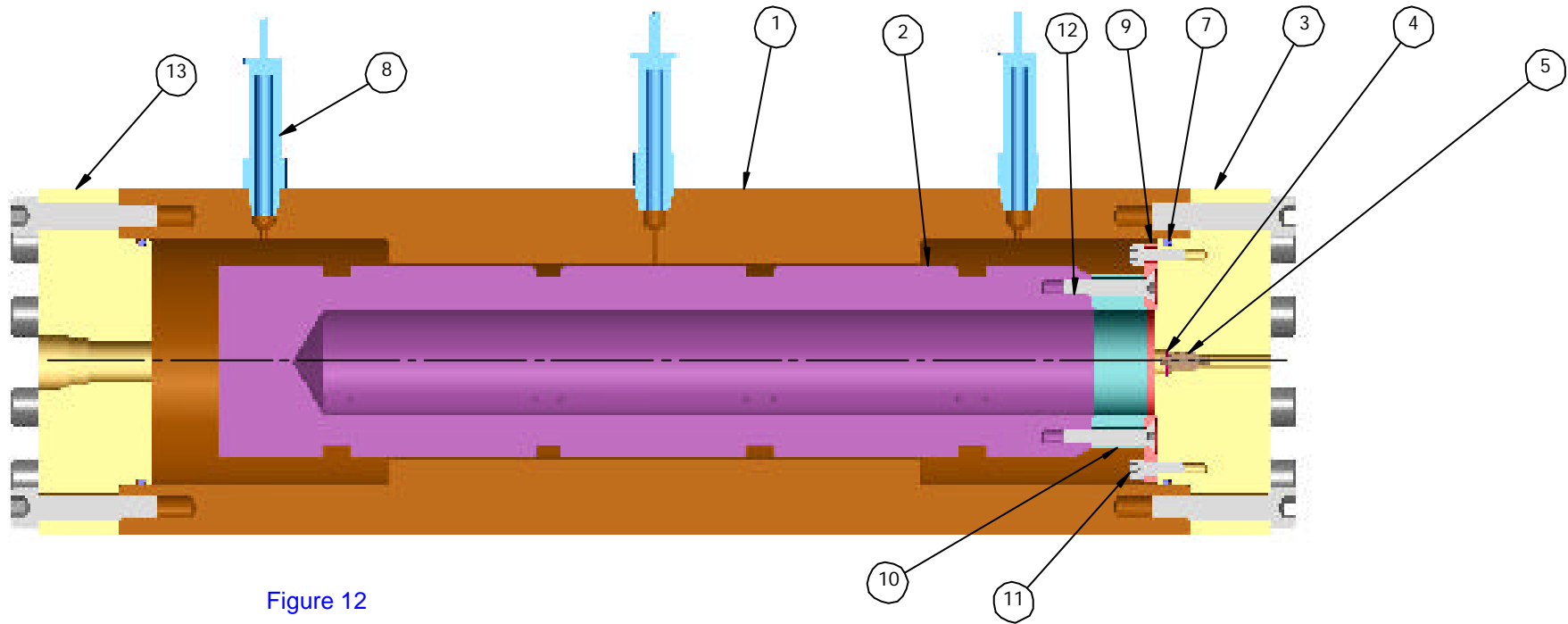


Figure 9: Schematic of AVD Tool

Figure 10: (Next page) Detail view of the adjustable damping element design

Figure 11:(Second following page) AVD Test Bench



RFV	DESC
A	INITIAL RELEASE

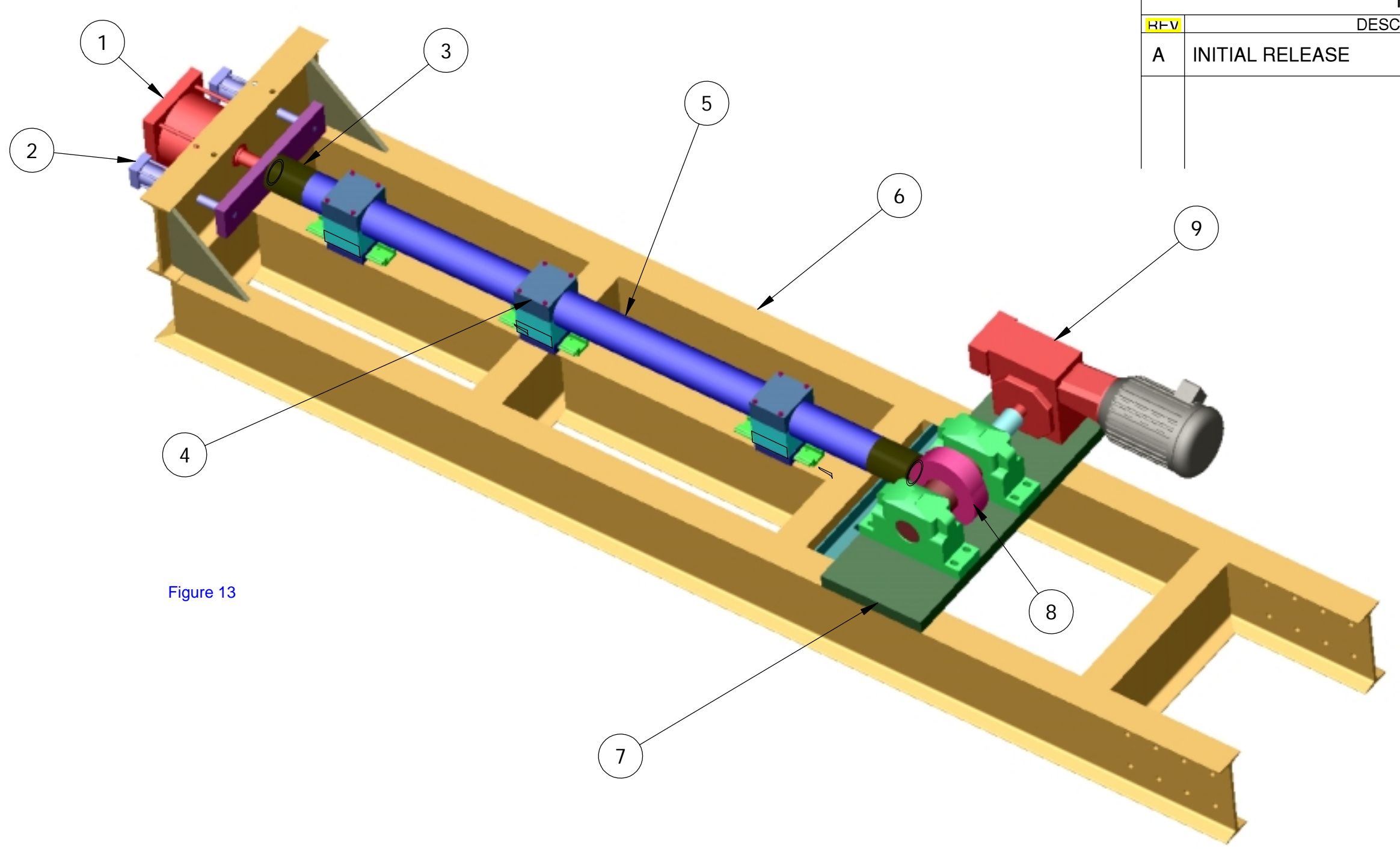


Figure 13

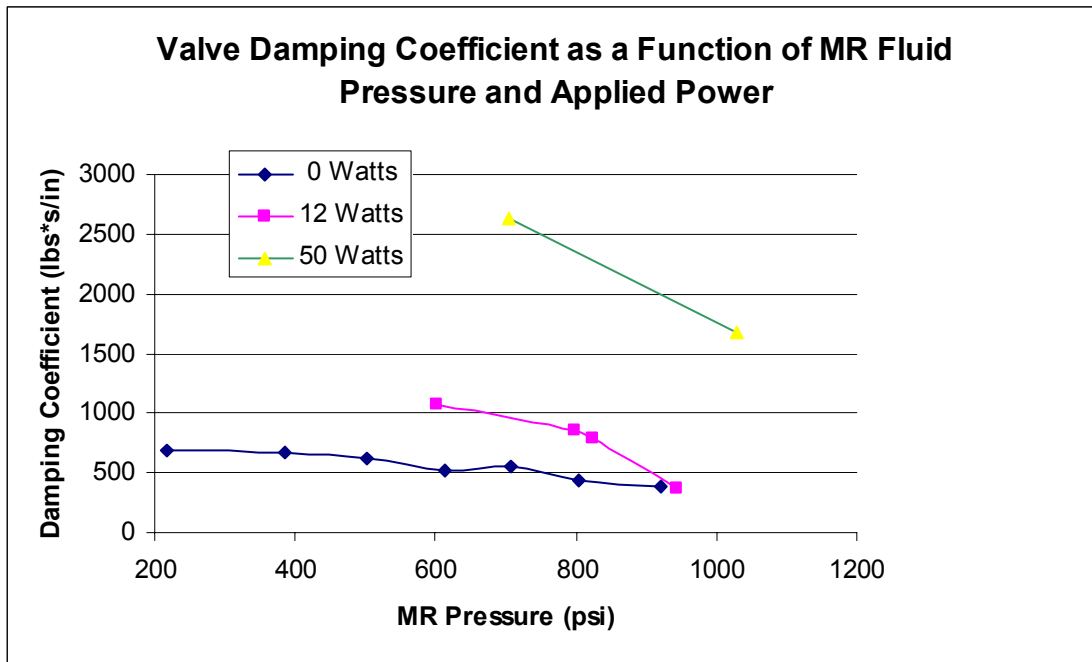


Figure 12: Variation of Damping Coefficient vs. Pressure and Power in Initial Testing

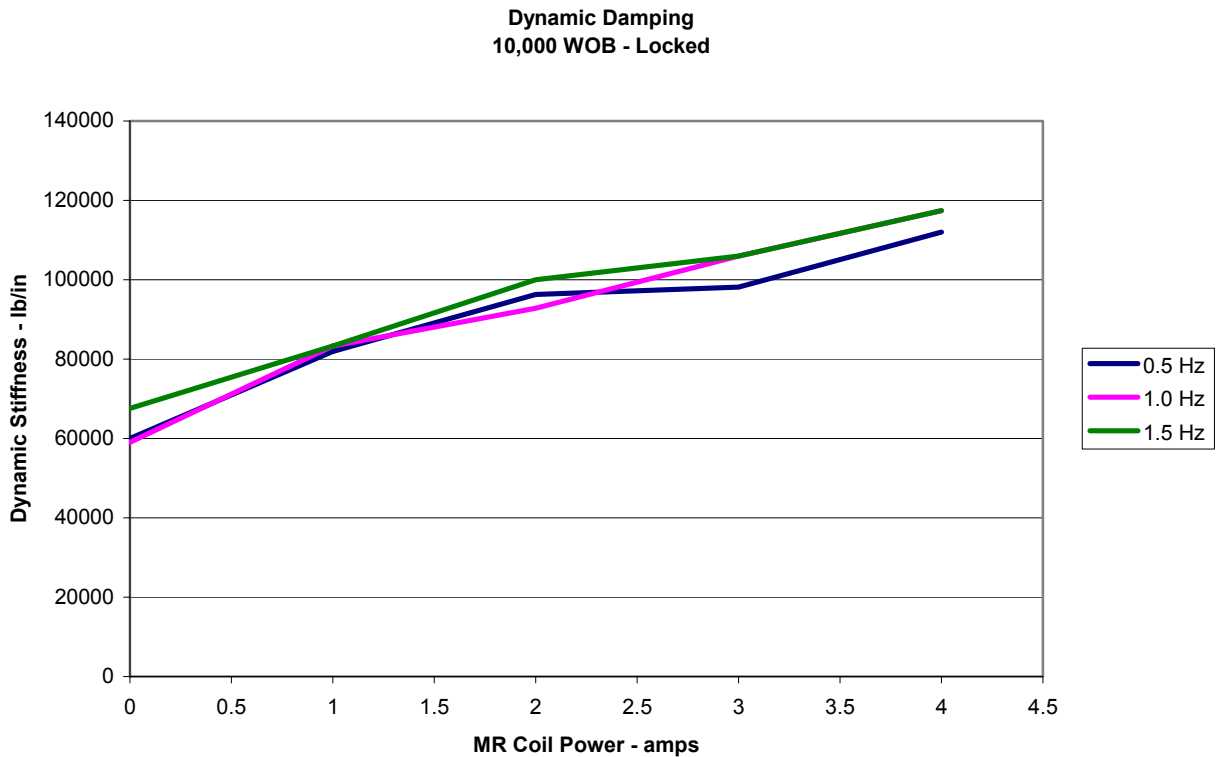


Figure 13: 10,000 lbs. WOB - AVD dynamic stiffness

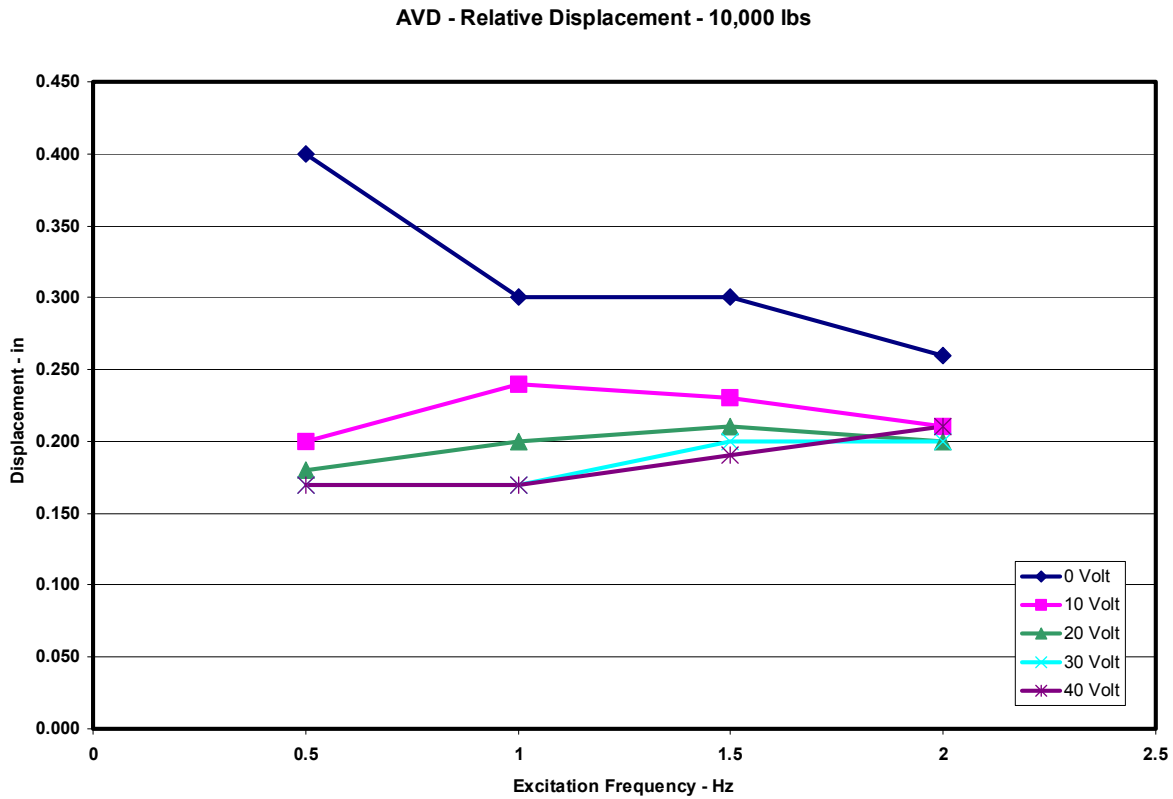


Figure 14: Maximum relative motion of the damper during testing

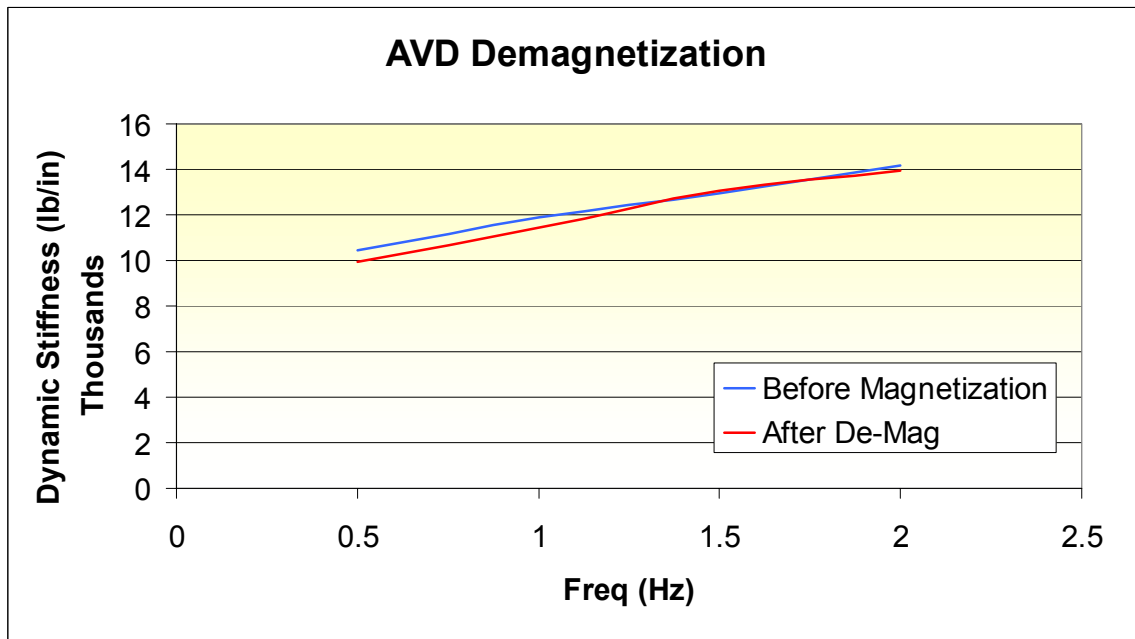


Figure 15: Effect of demagnetization of the dynamic stiffness of the AVD

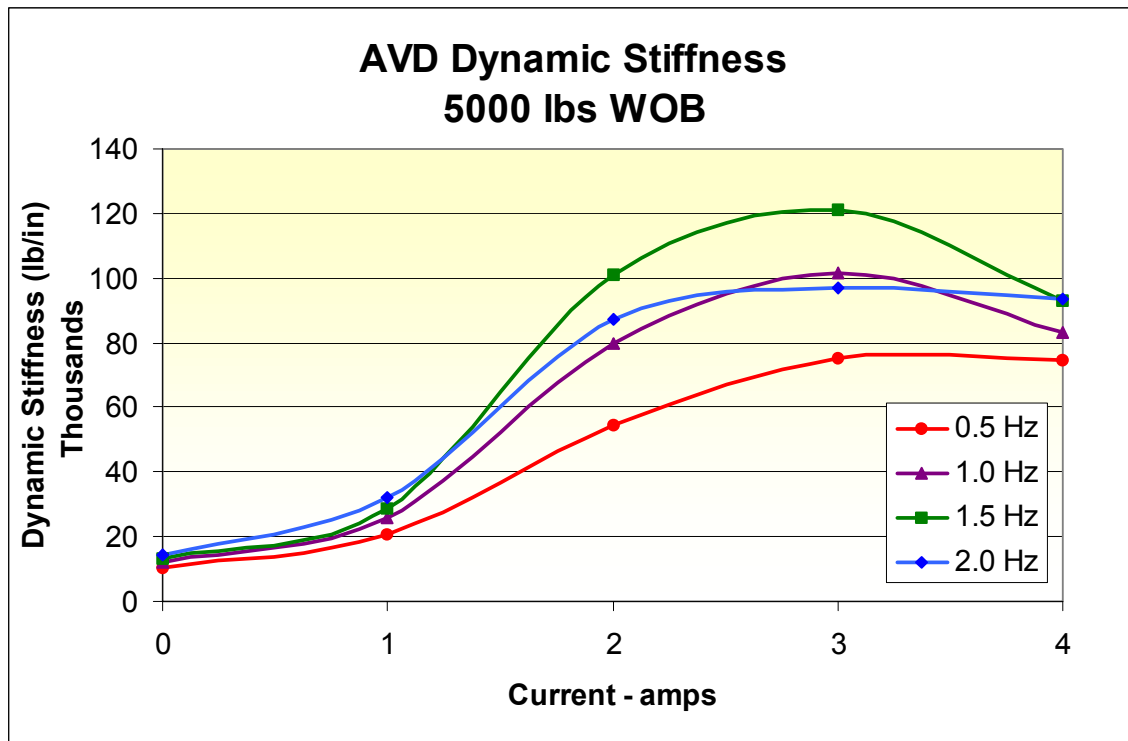


Figure 16: Dynamic stiffness of the AVD as a function of current and frequency, with demagnetization circuit